Direct method for phase retrieval from the intensity of cylindrical wave fronts

Kieran G. Larkin* and C. J. R. Sheppard

Department of Physical Optics, School of Physics, The University of Sydney, NSW 2006, Australia

Received October 6, 1998; revised manuscript received March 11, 1999; accepted March 12, 1999

The phase-retrieval problem for a physical system with strong support constraints is investigated. Propagation of an optical field in a system with no variation along one transverse axis results in cylindrical wave fronts. Scalar propagation in such systems is a purely two-dimensional process. We show that, given the optical intensity in a plane, the phase of the wave field can be calculated directly if the system has this special symmetry. The procedure relies on a simple geometric relation between the system pupil function (or angular spectrum) and the system optical transfer function in the Debye theory of scalar wave focusing. The inherent autocorrelation operation can be undone, and the phase directly retrieved, with a simple coordinate transformation. © 1999 Optical Society of America [S0740-3232(99)01307-1]

OCIS codes: 100.0100, 100.3190, 100.1830, 100.5070, 070.0070, 070.2590, 050.0050, 050.1960, 120.5060.

1. INTRODUCTION

Recently there has been some interest shown in the noninterferometric reconstruction of complex wave fields from intensity measurements.[1,2] At the same time, it has been shown that for partially coherent systems such reconstruction is not, in general, possible because different wave fields can exhibit identical intensity distributions.[3–5] The more restricted problem of finding the complex wave field corresponding to the three-dimensional (3D) intensity in a coherent system may be soluble by phase-retrieval techniques but is not directly soluble unless the phase variation is suitably constrained: Essentially, the transverse phase derivative must be slowly varying.[6,7]

We consider a particular subset of the general problem that is demonstrably soluble by a direct method. The particular subset considered is essentially an optical wave field with cylindrical symmetry. Such symmetry reduces the problem from three to two dimensions, resulting in a well-posed inverse problem. The resulting two-dimensional (2D) problem may be considered as a typical phase-retrieval problem with a very specific support constraint that is due to the wave equation. Phase retrieval in two dimensions results in a unique solution in most practical cases.[8–12] However, the calculation invariably relies on an iterative error-reducing algorithm originally proposed by Gerschberg and Saxton.[13] More recently, the convergence of the algorithm has been accelerated, but the method remains very sensitive to noise in the starting data.

The importance of support constraints in the avoidance of ambiguity is well known.[11,14] Using the very special support constraints of the wave equation, we have developed a direct method of phase retrieval from the intensity of a 2D coherent wave field. The solution presented is not just a theoretical curiosity inasmuch as systems with the required symmetry occur in slab waveguides and slit illumination systems.

It is, perhaps, surprising to note that a significant body of research—broadly contained under the description diffraction tomography—has covered much of the background to the theory presented in this paper yet has not proposed such a method before (as far as we can ascertain from the available literature). So, for example, the circular arc support constraint is fundamental to the Fourier representation of optical tomographic sampling.[15,16] However, most tomographic or inverse optical methods explicitly require measurement or estimation of the coherent field as input data for the backprojection or the backpropagation reconstruction algorithms.[15,17–19] Therefore, in practice, a preliminary step of phase retrieval from intensity measurements is required. A number of phase-retrieval methods, such as interferometric (or holographic) measurement,[20–22] iterative retrieval from single intensity planes, and direct retrieval from two intensity planes[19,21] (more recently of interest to adaptive optics), have been proposed. It may very well be that the number of sampled intensity points required by our proposed method was previously considered so extreme that any such solution would be considered impractical. The comparable methods in two dimensions require only one or two lines of sampled intensities, whereas we require a sequence of lines covering a 2D patch. The collection of such a 2D data set is not considered here, but it is not inconceivable that a carefully designed optical imaging system could collect all the required intensity data simultaneously. Not all tomographic systems require coherent field data: For example, the 3D reconstruction of fluorescent stained objects is essentially an incoherent process,[23–25] although objects with varying refractive index do require phase information associated with the optical field.[26]

In the following sections we outline the Fourier representation of the problem, which then leads to a convenient coordinate transformation that converts the problem into estimation of a 2D separable function. Computational aspects are considered, and an experimen-

tal (computer simulation) verification appears in the later sections before an overall conclusion is drawn.

2. FOURIER REPRESENTATION OF THE PROBLEM

Initially we assume that we have access to the field intensity at all points in the x–z plane. Details of sampling and the limited extent of measurements are ignored in this preliminary investigation.[27] The assumption of cylindrical symmetry results in a field independent of the y coordinate. We also assume a scalar, quasi-monochromatic optical field E propagating in the z direction with a field intensity I given by

$$I(x,y,z) \equiv |E(x,y,z)|^2 = |f(x,y,z)|^2 = I(x,z) = |f(x,z)|^2. \quad (1)$$

The notation for the intensity function $f(x,y,z) = I(x,y,z)$ is used here for convenience. We also assume that the field considered is sufficiently far from apertures or other obstructions for near-field contributions to be negligible. In such a case the Debye approximation is appropriate if the Fresnel number of the system is large. The propagation medium is a linear, uniform, and isotropic medium with refractive index 1. Under such conditions the field function $f(x,y,z)$ satisfies a simple wave equation—more specifically, the Helmholtz equation:

$$\nabla^2 f(x,y,z) + k^2 f(x,y,z) = 0. \quad (2)$$

The wave number and the wavelength are related, as usual, by $k\lambda = 2\pi$. It is worth noting that the approximations used are not valid for high-aperture optical systems unless the vectorial components are explicitly included.[28] We are interested in the Fourier transform of the field function (sometimes known as the angular spectrum) defined for the spatial-frequency coordinates (m, n, s):

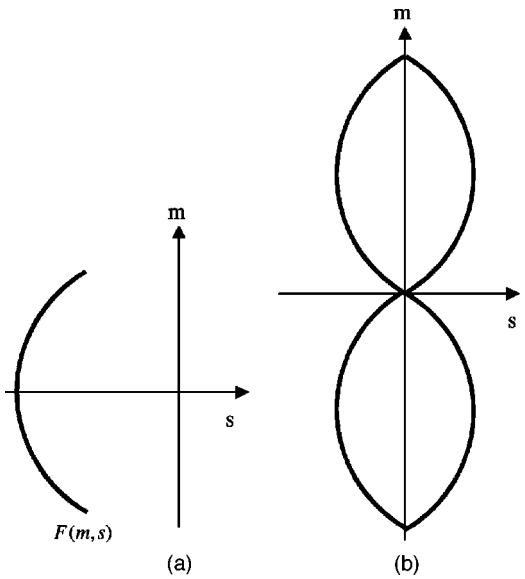

Fig. 1. Regions of support for (a) the pupil function $F(m,s)$ and (b) its autocorrelation.

$$F(m,n,s) = \int\int\int f(x,y,z) \times \exp[-2\pi i(mx + ny + sz)]\,dx\,dy\,dz. \quad (3)$$

Fourier transforming Eq. (2) reveals that the transform of the field exists only on the surface of the Ewald sphere[29]:

$$F(m,n,s)[k^2 - (2\pi)^2(m^2 + n^2 + s^2)] = 0. \quad (4)$$

The function $F(m,n,s)$ is sometimes referred to as the 3D pupil function or, more generally, as the angular spectrum.

The lack of variation of $f(x,y,z)$ in the y direction, i.e., the cylindrical symmetry, ensures the further restriction of F to an arc of a circle, radius $1/\lambda$, in the (m, s) plane:

$$F(m,n,s)[1 - \lambda^2(m^2 + n^2 + s^2)]\delta(s) = 0 = F(m,s)[1 - \lambda^2(m^2 + s^2)]. \quad (5)$$

Initially we have only measurements of the field intensity (modulus squared of the field), which has a Fourier transform that is the autocorrelation of $F(m,s)$. If $F(m,s)$ exists only on a circular arc, as shown in Fig. 1(a), then its autocorrelation exists only on a bow- (or petal-) shaped region bounded by similar circular arcs,[30] as shown in Fig. 1(b). In this case the arc [Fig. 1(a)] corresponds to the angular spectrum of an optical wave propagating from left to right.

3. COORDINATE TRANSFORM

When considering the autocorrelation of a function with support on a circular arc, it is more convenient to use a coordinate measuring the angular position along the arc. Figure 2 shows the angular parameter defined by the following coordinate transform:

$$m\lambda = \sin\theta_1 - \sin\theta_2$$
$$s\lambda = \cos\theta_2 - \cos\theta_1. \quad (6)$$

This coordinate transform is essentially the same as that adopted by Sheppard[30] to describe microscope imaging of 3D objects in transmission.

In Eq. (3) the Fourier transform of the wave field $f(x,z)$ is the 2D angular spectrum $F(m,s)$ and is directly analogous to the system pupil function. By transforming to the new coordinate system of Eqs. (6) we obtain the pupil function $\tilde{F}(\theta)$ parameterized by the angle θ. Similarly, we can consider the transform of the 2D intensity pattern $g(x,z) = I(x,z) = |f(x,z)|^2$:

$$G(m,s) = \int\int g(x,z)\exp[-2\pi i(mx + sz)]\,dx\,dz = \int\int F(m',s')F^*(m' - m, s' - s)\,dm'\,ds'. \quad (7)$$

The above function corresponds to the 3D optical transfer function first proposed by Frieden[31] for the analysis of optical imaging systems. Interestingly, the problem for cylindrical imaging was considered by Mertz in 1965.[32] Again, the resulting function can be transformed by use of

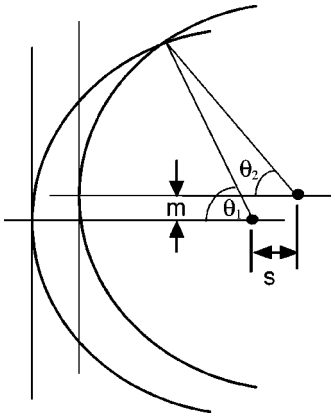

Fig. 2. Spatial-frequency coordinate system and angular coordinate system.

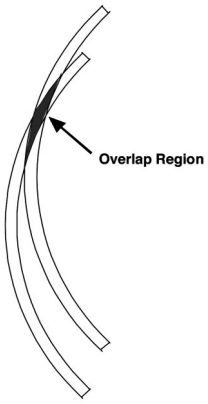

Fig. 3. Overlap region in the autocorrelation of $F(m, s)$. Note the rhombic shape.

Eqs. (6) to give $\tilde{G}(\theta_1, \theta_2)$. The omission of the wavelength parameter λ in the following analysis is equivalent to having *a priori* knowledge of the exact value. Figure 2 represents the overlap of two arcs as they are correlated. Figure 3 shows more detail for the general case of arcs with finite thickness (i.e., nonzero bandwidth). The overlap area is related to the angular difference $\theta_1 - \theta_2$. Treating the arc-supported functions as generalized functions then gives the simple overlap integral

$$\tilde{G}(\theta_1, \theta_2) = \frac{\tilde{F}(\theta_1)\tilde{F}^*(\theta_2)}{|\sin(\theta_1 - \theta_2)|}. \tag{8}$$

Clearly, $\tilde{G}(\theta_1, \theta_2)$ is a separable function of $\tilde{F}(\theta_1)$ and $\tilde{F}(\theta_2)$ that occupies a square region, $-\Theta < \theta_1 < \Theta$ and $-\Theta < \theta_2 < \Theta$, in which the optical system semiaperture is defined by the angle Θ. A similar analysis by Sheppard *et al.*[33] derives a square region with an upper triangular portion related to a convolution rather than a correlation. Equation (8) is effectively the recipe for deconvolution of $G(m, s)$. The constraints of the wave equation have ensured that the autocorrelation involves only the overlap of two points (located at θ_1 and θ_2), which allows subsequent separation of the simple product $\tilde{F}(\theta_1)\tilde{F}^*(\theta_2)$. Equation (8) contains a singularity at $\theta_1 = \theta_2$. The singularity occurs only in the limit of monochromaticity. In practice, the near singularity affects the noise sensitivity of phase calculations in the region $\theta_1 \approx \theta_2$, as shown in Section 4.

4. COMPUTATIONAL PROCEDURE

The preceding sections have outlined an intuitively inspired method of undoing the autocorrelation associated with the modulus-squaring operation. We now outline the actual computation scheme developed to numerically model the process. In the continuous domain the combination of Eqs. (6) and (7) gives

$$\begin{aligned} G(m, s) &= \tilde{G}(\theta_1, \theta_2) \\ &= \int\int g(x, z)\exp\{-(2\pi i/\lambda)[(\sin\theta_1 - \sin\theta_2)x \\ &\quad + (\cos\theta_2 - \cos\theta_1)z]\}\mathrm{d}x\,\mathrm{d}z. \end{aligned} \tag{9}$$

From this the underlying angular spectrum $\tilde{F}(\theta)$ is available in a 2D separable form:

$$\tilde{F}(\theta_1)\tilde{F}^*(\theta_2) = |\sin(\theta_1 - \theta_2)|\tilde{G}(\theta_1, \theta_2). \tag{10}$$

The main problem in the computation is in the interpolation intrinsic to the coordinate transform of Eqs. (6), illustrated in Fig. 4. The coordinate transformation occurs after the initial step of Fourier transforming the measured intensity distribution. Typically, the Fourier transformation is performed as a discrete fast Fourier transform with all the speed advantages that this implies. However, by utilizing a discrete Fourier transformation with nonuniformly spaced indices, we can combine both the Fourier and the coordinate transformations into one. We lose the redundancy properties needed for the fast Fourier transform decomposition, but we gain perfect sinc-based (band-limited) interpolation for all the new coordinate indices. The discrete Fourier transform for estimating the angular spectrum of $g(x, z)$ is as follows:

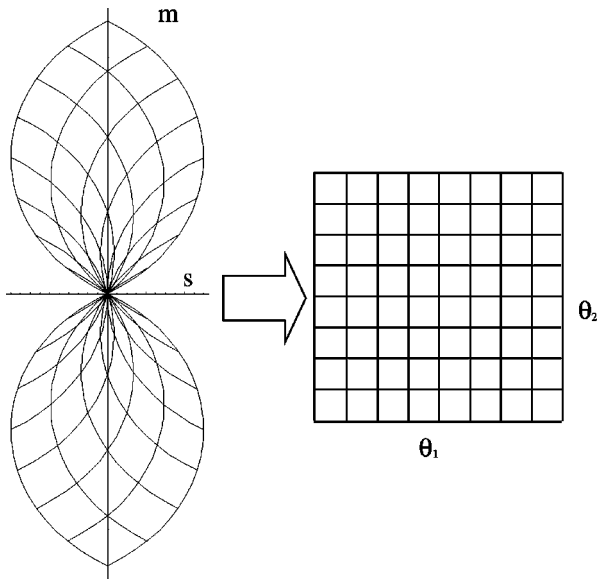

Fig. 4. Effect of coordinate transformation for a typical grid pattern.

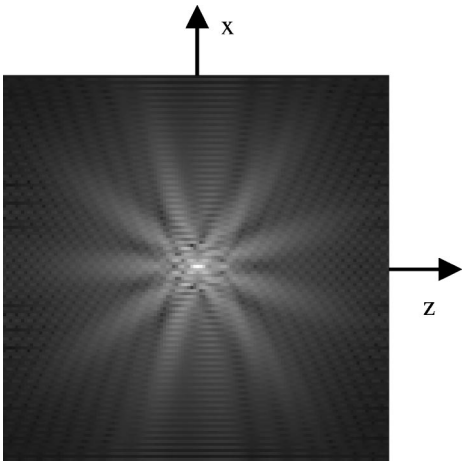

Fig. 5. Gray-scale plot of a typical intensity pattern. The quartic root of the intensity is displayed to enhance low-level features of interest. This particular pattern corresponds to the focal region of a phase-aberrated cylindrical wave.

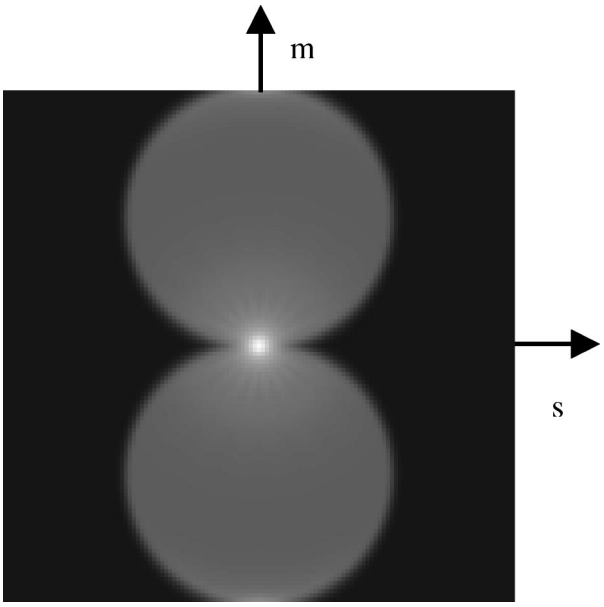

Fig. 6. Gray-scale plot of the modulus of the Fourier-transformed intensity, $|G(m, s)|$. The gray scale is nonlinear to enhance low-level features of interest. The predicted correlation petal-shaped outline is clearly shown. Note that $G(m, s)$ is, in general, complex.

$$G_{\rho,\sigma} = G[\rho/(N\Delta),\sigma/(N\Delta)] = \frac{\Delta^2}{N}\sum_{q=0}^{N-1}\sum_{p=0}^{N-1} g(p\Delta, q\Delta)\exp[2\pi i(p\rho + q\sigma)/N], \tag{11}$$

where $g_{p,q} = g(p\Delta, q\Delta)$ and both p and q are integers representing the intensity g on a square grid of sample points separated by Δ. Typical examples of $g(x, z)$ and $|G(m, s)|$ are shown in Figs. 5 and 6. Both Figs. 5 and 6 represent the functions as gray levels in an image. The gray-level scales are nonlinear to enhance the low values and to make salient detail visible. Equation (9) represents the function G on a square grid with integer indices ρ and σ. Combining the coordinate transform, so that the transform is evaluated at intersample points, we get the following equation:

$$\tilde{F}_\alpha \tilde{F}_\beta{}^* = \tilde{G}(\alpha, \beta) = \frac{\Delta^2}{N}\left|\sin\left[\frac{2\pi(\alpha - \beta)}{N}\right]\right| \times \sum_{p=-(N/2)+1}^{(N/2)-1}\sum_{p=-(N/2)+1}^{(N/2)-1} g_{p,q} \times \exp\left(\frac{2\pi i L}{N}\left\{p\left[\cos\left(\frac{2\pi\alpha}{N}\right) - \cos\left(\frac{2\pi\beta}{N}\right)\right] + q\left[\sin\left(\frac{2\pi\beta}{N}\right) - \sin\left(\frac{2\pi\alpha}{N}\right)\right]\right\}\right). \tag{12}$$

The discrete form of the coordinate transform that we have chosen in this case has the following scaling:

$$\theta_1 = \frac{2\pi\alpha}{N}, \qquad \theta_2 = \frac{2\pi\beta}{N}, \qquad \frac{1}{\lambda} = \frac{L}{N\Delta}, \tag{13}$$

which gives $N - 1$ samples over the range $-N/2 + 1 \leqslant \alpha < N/2 - 1$, where α is the integer. A similar relation applies to β, so that we finally map into a 2D grid with angular coordinates symmetrically spanning 2π in each direction.

Once we have calculated $\tilde{G}(\theta_1, \theta_2)$, we can apply a variety of simple statistical techniques to extract $\tilde{F}(\theta)$, depending on our models of expected noise in the system. So, for example (in the noise-free case), we can normalize the function $\tilde{G}(\theta_1, \theta_2)$, removing the singularity in the process, and then integrating over one coordinate:

$$\int_{-\Theta}^{\Theta} \tilde{G}(\theta_1, \theta_2)|\sin(\theta_1 - \theta_2)|\mathrm{d}\theta_1 = \tilde{F}(\theta_1)\int_{-\Theta}^{\Theta} \tilde{F}(\theta_2)\mathrm{d}\theta_2. \tag{14}$$

Hence both the amplitude and the phase (i.e., the complex amplitude) of $\tilde{F}(\theta)$ can be found for a coherent field. Alternatively, methods (such as correlation or matched filtering) that exploit the large degree of redundancy in the 2D separable function can be utilized. In systems with partial coherence a unique phase cannot be associated with each part of the angular spectrum, but some overall statistical parameters may be calculated in a similar manner.

5. EXPERIMENTAL VERIFICATION

A preliminary verification of the method was implemented as follows:

1. A 2D pupil function (angular spectrum) with constant magnitude and known phase variation was generated; see Fig. 7.

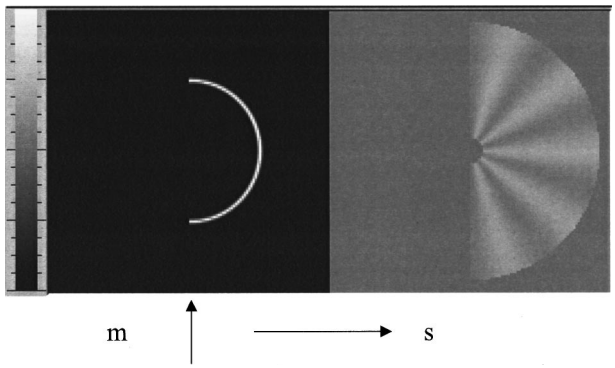

Fig. 7. Gray-scale plot of the initial angular spectrum $F(m, s)$ as a magnitude (left-hand-side) and a phase (right-hand-side) component. The gray scales are linear in this case. Note that the circular arc subtends π rad and has been given a narrow Gaussian profile to reduce line-aliasing artifacts. The imposed phase modulation has a sinusoidal form with five periods over the arc length. The linear gray scale is shown at the far left.

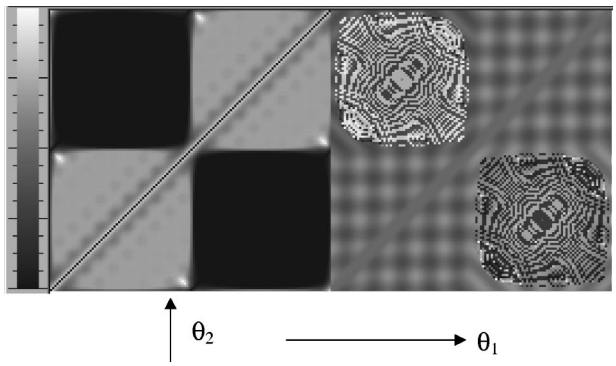

Fig. 8. Gray-scale plot of $\tilde{F}(\theta_1)\tilde{F}^*(\theta_2)$ from the direct phase-retrieval algorithm of Eq. (12). The magnitude is on the left; the phase, on the right. Note that the magnitude is near constant (light gray) over the upper right-hand quadrant corresponding to the range $-\pi/2 < \theta_{1,2} < \pi/2$ in this implementation. The phase component clearly shows the five-period grid variation that we expect in this example. The patterns have Hermitian symmetry and could be adequately defined over a region half this area.

2. The corresponding 2D field pattern was calculated by use of the fast Fourier transform in the Debye approximation.

3. The corresponding modulus-squared (intensity) pattern was calculated; see Fig. 5.

4. The direct phase-retrieval algorithm embodied in Eq. (12) was applied to the 2D intensity pattern, resulting in the magnitude and phase patterns shown in Fig. 8.

5. Integration along the θ_2 direction was used to estimate the phase component of $\tilde{F}(\theta_1)$ according to Eq. (14).

6. Steps 3–6 were repeated for the same intensity distribution with uniform random noise added.

The pertinent experimental details are as follows:

1. The angular spectrum used (Fig. 7) has a radius of 32 pixels in a sampled region of 128 × 128 pixels. The circular arc has a narrow Gaussian profile to reduce line-aliasing artifacts. The spectrum has an imposed phase variation of sinusoidal form with five periods over the semicircular arc. Note that the five-period phase function is not representable by a low-order polynomial and may be expected to defeat phase-retrieval schemes that inherently require slow phase variation to succeed.

2. Detailed sampling requirements will be investigated in subsequent publications. In this instance we have chosen approximately 4 pixels/fringe, giving 32 fringes over the 128-pixel frame. The resulting intensity distribution just satisfies the Nyquist sampling criterion.

3. Dynamic range and measurement quantization are also important, but such issues are avoided in this example with the use of floating-point numbers.

4. The direct phase-retrieval algorithm requires operations of order N^4 to compute for a $N \times N$ image. In this case $N = 128$, and approximately 10^9 floating-point operations are required.

5. More-sophisticated, statistically based methods can be used to extract the 2D separable function given by Eq. (12). However, the simplistic analysis of Eq. (14) gives results as shown in Fig. 9. In fact, there is some error in the range of the recovered phase: The calculation gives a ±0.43-rad range, whereas the simulation actually used a

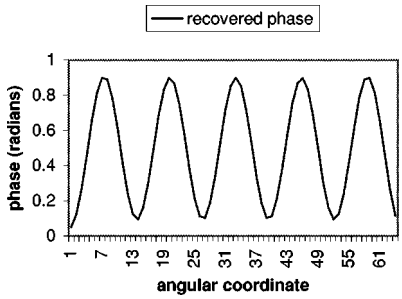

Fig. 9. Phase profile recovered by use of Eq. (14). The predicted five-period sinusoid is clear. The 64 samples cover the angular coordinate range $-\pi/2 < \theta_1 < \pi/2$.

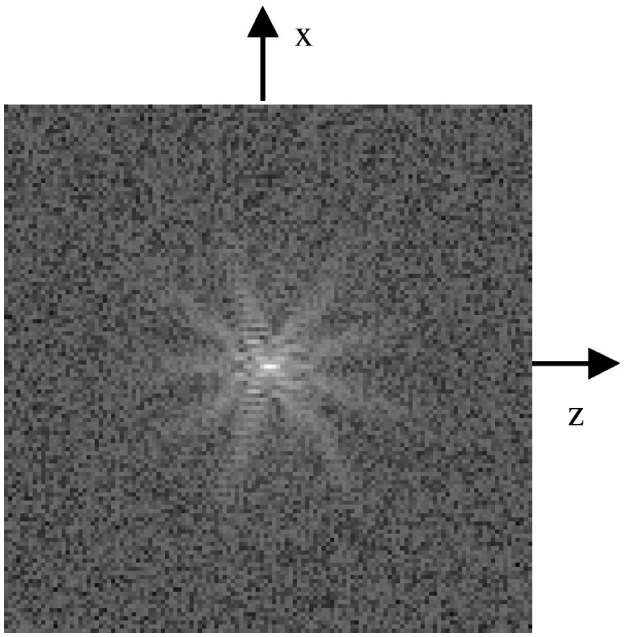

Fig. 10. Gray-scale plot of an intensity pattern with a uniform random noise. The random noise range is ±2% of the peak intensity. The quartic root of the intensity is displayed to enhance low-level features of interest.

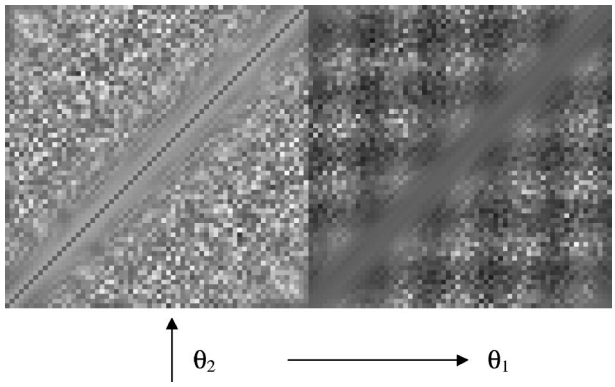

Fig. 11. Gray-scale plot of $\tilde{F}(\theta_1)\tilde{F}^*(\theta_2)$ from the direct phase-retrieval algorithm applied to the noisy intensity map. The magnitude (left-hand-side) and phase (right-hand-side) areas shown correspond to the top right-hand quadrants in Fig. 8.

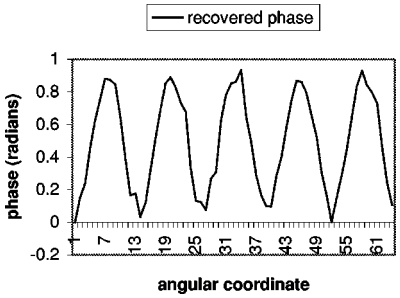

Fig. 12. Phase profile recovered from the noisy intensity map. Again the predicted five-period sinusoid is clear. The 64 samples cover the angular coordinate range $-\pi/2 < \theta_1 < \pi/2$.

range of ± 0.50 rad, implying a degree of attenuation in the reconstruction. Because the 1D information is uniformly spread over two dimensions as a separable function, there is a large degree of degeneracy in the output, which could be utilized to minimize noise effects. Alternatively, only a small section of the output shown in Fig. 8 needs to be calculated to estimate the phase when noise is not a concern. Values along the diagonal of Fig. 8 corresponding to $\alpha = \beta$ have a zero weight from Eq. (12) and cannot contribute useful amplitude or phase information.

6. Uniform random noise with a range equivalent to $\pm 2\%$ of the peak intensity value was added to the original intensity distribution, and the direct phase-retrieval method was repeated. This is a significant amount of noise compared with the likely quantization noise, for example. Figure 10 shows the noise dominating the intensity distribution in all regions more than a few wavelengths from the peak intensity. After applying Eq. (12) we obtain the separable function shown in Fig. 11. The noise effects appear to be well spread, and the correct underlying phase is still visible. Application of the simple projection of Eq. (14) gives the pupil phase function in Fig. 12. The original pupil phase is still close to its correct form, with some attenuation, as before. Further simulations are needed to better quantify this effect.

6. CONCLUSIONS

We have presented a direct method for calculating the phase of a wave field in a cylindrically symmetric optical system, and the initial simulation results are in close agreement with predictions. The method relies on the Fourier transform of the wave-field intensity, which is then remapped into a new coordinate system. The combination of Fourier transform and remapping conveniently overcomes interpolation difficulties but results in a significant computational load. Much work remains to fully characterize the method and explore its limitations, especially in the presence of noise, although initial simulations indicate a significant insensitivity to additive intensity noise. From the point of view of phase retrieval in two dimensions, there are some unusual support constraints with physical significance, and a comparison with iterative retrieval schemes may prove illuminating. The method is applicable to certain optical systems, such as the light emitted from slab waveguides and other anamorphic systems. Measurements required for characterizing such systems could be obtained quickly by the use of a 2D photodetector array in a suitably arranged imaging system. The method presented is an interesting alternative to conventional interferometric phase-measurement methods.

ACKNOWLEDGMENTS

The authors thank Michael Oldfield for writing the computer code to evaluate Eq. (12).

*Present address, Canon Information Systems Research Australia, 1 Thomas Holt Drive, North Ryde, NSW 2113, Australia.

REFERENCES

1. M. G. Raymer, M. Beck, and D. F. McAlister, "Complex wavefield reconstruction using phase-space tomography," Phys. Rev. Lett. **72**, 1137–1140 (1994).
2. D. F. McAlister, M. Beck, L. Clarke, A. Mayer, and M. G. Raymer, "Optical phase retrieval by phase-space tomography and fractional-order Fourier transforms," Opt. Lett. **20**, 1181–1183 (1995).
3. E. Collett and E. Wolf, "Is complete spatial coherence necessary for the generation of highly directional light beams?" Opt. Lett. **2**, 27–29 (1978).
4. F. Gori, M. Santarsiero, and G. Guattari, "Coherence and the spatial distribution of intensity," J. Opt. Soc. Am. A **10**, 673–679 (1993).
5. T. E. Gureyev, A. Roberts, and K. A. Nugent, "Partially coherent fields, the transport-of-intensity equation, and phase uniqueness," J. Opt. Soc. Am. A **12**, 1942–1946 (1995).
6. M. R. Teague, "Irradiance moments: their propagation and use for unique retrieval of phases," J. Opt. Soc. Am. A **72**, 1199–1209 (1982).
7. M. R. Teague, "Deterministic phase retrieval: a Green's function solution," J. Opt. Soc. Am. **73**, 1434–1441 (1983).
8. A. Walther, "The question of phase retrieval in optics," Opt. Acta **10**, 41–49 (1962).
9. I. M. Bruck and L. G. Sodin, "On the ambiguity of the image restoration problem," Opt. Commun. **30**, 304–308 (1979).
10. J. R. Fienup, "Reconstruction of an object from the modulus of its Fourier transform," Opt. Lett. **3**, 27–29 (1978).
11. M. A. Fiddy, B. J. Brames, and J. C. Dainty, "Enforcing irreducibility for phase retrieval in two dimensions," Opt. Lett. **8**, 96–98 (1983).
12. R. H. T. Bates, "Fourier phase problems are uniquely solvable in more than one dimension: underlying theory," Optik **61**, 247–262 (1982).

13. R. W. Gerschberg and W. O. Saxton, "A practical algorithm for the determination of phase from image and diffraction plane pictures," Optik **35**, 237–246 (1972).
14. J. R. Fienup, "Phase retrieval using boundary conditions," J. Opt. Soc. Am. A **3**, 284–288 (1986).
15. M. Kaveh and M. Soumekh, "Computer-assisted diffraction tomography," in *Image Recovery: Theory and Application*, H. Stark, ed. (Academic, Orlando, Fla., 1987), pp. 369–413.
16. M. H. Maleki, A. J. Devaney, and A. Schatzberg, "Tomographic reconstruction from optical scattered intensities," J. Opt. Soc. Am. A **9**, 1356–1363 (1992).
17. A. J. Devaney, "A filtered backpropagation algorithm for diffraction tomography," Ultrason. Imaging **4**, 336–350 (1982).
18. H. P. Baltes, "Introduction," in *Inverse Source Problems*, H. P. Baltes, ed. (Springer-Verlag, Berlin, 1978), pp. 1–10.
19. H. A. Ferweda, "The phase reconstruction problem for wave amplitudes and coherence functions," in *Inverse Source Problems*, H. P. Baltes, ed. (Springer-Verlag, Berlin, 1978), pp. 13–38.
20. E. Wolf, "Three-dimensional structure determination of semi-transparent objects from holographic data," Opt. Commun. **1**, 153–156 (1969).
21. M. H. Maleki and A. J. Devaney, "Phase retrieval in inverse scattering," in *Inverse Problems in Scattering and Imaging*, M. A. Fiddy, ed., Proc. SPIE **1767**, 398–408 (1992).
22. M. H. Maleki and A. J. Devaney, "Holographic techniques for inverse scattering and tomographic imaging," in *Practical Holography VIII*, S. A. Benton, ed., Proc. SPIE **2176**, 184–194 (1994).
23. N. Streibl, "Three-dimensional imaging by a microscope," J. Opt. Soc. Am. A **2**, 121–127 (1985).
24. P. J. Shaw, D. A. Agard, Y. Hiraoka, and J. W. Sedat, "Tilted view reconstruction in optical microscopy," Biophys. J. **55**, 101–110 (1989).
25. C. J. Cogswell, K. G. Larkin, and H. U. Klemm, "Fluorescence microtomography: multiangle image acquisition and 3D digital reconstruction," in *Three-Dimensional Microscopy: Image Acquisition and Processing III*, C. J. Cogswell and G. S. Kino, eds., Proc. SPIE **2655**, 109–115 (1996).
26. T. C. Wedberg and J. Stamnes, "Experimental examination of the quantitative imaging properties of optical diffraction tomography," J. Opt. Soc. Am. A **12**, 493–500 (1995).
27. In practice we have access only to discretely sampled measurements over a finite region of space. It is a straightforward procedure to include these limitations and the computation artifacts that ensue. The main effect, which is due to the finite area, is a blurring in the angular spectrum domain.
28. C. J. R. Sheppard and K. G. Larkin, "Vectorial pupil functions and vectorial transfer functions," Optik **107**, 79–87 (1997).
29. C. W. McCutchen, "Generalized aperture and the three-dimensional diffraction image," J. Opt. Soc. Am. **54**, 240–244 (1964).
30. C. J. R. Sheppard, "The spatial frequency cut-off in three-dimensional imaging," Optik **72**, 131–133 (1986).
31. B. R. Frieden, "Optical transfer of the three-dimensional object," J. Opt. Soc. Am. **57**, 56–66 (1967).
32. L. Mertz, *Transformations in Optics* (Wiley, New York, 1965).
33. C. J. R. Sheppard, T. J. Connolly, and M. Gu, "Scattering by a one-dimensional rough surface, and surface profile reconstruction confocal imaging," Phys. Rev. Lett. **70**, 1409–1412 (1993).